



PVD-Aided Consolidation with Spatial Variations in Soil Properties and Initial Excess Pore Pressure

Amitava Chakraborti¹ · Dipanjan Basu² · Sibapriya Mukherjee¹ · Gupinath Bhandari¹

Received: 28 June 2021 / Accepted: 28 January 2022 / Published online: 1 March 2022
 © The Author(s), under exclusive licence to Springer Nature Switzerland AG 2022

Abstract

Analytical solutions for determining the degree of consolidation of clayey soils caused by the installation of prefabricated vertical drains (PVDs) are developed by considering the variations of initial excess pore pressure and soil properties with depth. The PVD is assumed to be installed in a clayey deposit with multiple layers, and the effect of soil disturbance caused by PVD installation is considered in the analysis. The analytical solutions are developed with the assumptions of equal-strain consolidation and continuity of flow that follow Darcy's law. These closed-form solutions are applicable for different cases that are expected to commonly occur in real field problems. It is observed based on parametric studies that different spatial variations of coefficient of consolidation and initial excess pore pressure impact the rate of consolidation differently. A numerical example is presented that demonstrates the use of the developed solutions.

Keywords Geosynthetics · Consolidation · Clay · Flow · Drain · Ground improvement · Multi-layered soil · Analytical solution

List of Symbols

d_w, d_t	PVD width and thickness (m)	k_{sm}, k_{tr}, k_c	Hydraulic conductivities in the smear, transition, and undisturbed zones (m/s)
p	Number of soil layers	$r_{m,eq}$	Equivalent mandrel radius (m)
r_d, r_c, r_{sm}, r_{tr}	Radii of drain, unit cell, smear zone, and transition zone (m)	β, β_z	Degree of disturbance in the smear zone
H_i	Thickness of the i th layer (m)	c_{h0}	Spatially constant part coefficient of consolidation (m^2/s)
L_d, s	Length and spacing of drain (m)	c_{h1}	Spatially constant part coefficient of consolidation
k	Hydraulic conductivity (m/s)	t	Time (s)
m_v	Coefficient of compressibility (kPa) ⁻¹	T	Time factor
c_h	Coefficient of consolidation (m^2/s)	T_0	Spatially constant part of time factor
\bar{u}_0	Initial excess pore pressure (kPa)	T_1	Spatially varying part of time factor
r	Radial distance (m)	$\bar{u}_{top}^{(i)}$	Initial excess pore pressure at the top of the i th layer (kPa)
z	Depth from ground surface (m)	$\bar{u}_{sl}^{(i)}$	Spatially varying part of initial excess pore pressure
		$\bar{u}_{L_d/2}$	Initial excess pore pressure at a depth $L_d/2$ (kPa)
		$u_{sm} _z, u_{tr} _z, u_c _z$	Excess pore pressures in the smear, transition, and undisturbed zones (kPa)
		$k_{c,z}, k_{sm,z}$	Hydraulic conductivities of undisturbed zone and smear zone at depth z (m/s)
		ε_v	Uniform vertical strain in the unit cell
		n, m, q	Ratios of parameters describing dimensions of unit cell, PVD and disturbed zone

✉ Dipanjan Basu
 dipanjan.basu@uwaterloo.ca

Amitava Chakraborti
 c_amitava2002@yahoo.co.in

Sibapriya Mukherjee
 sibapriya.mukherjee@gmail.com

Gupinath Bhandari
 g.bhandari.ju@gmail.com

¹ Department of Civil Engineering, Jadavpur University, Kolkata 700 032, India

² Department of Civil and Environmental Engineering, University of Waterloo, Waterloo, ON N2L 3G1, Canada

μ, μ_z	Parameters that depend on the unit cell geometry and soil disturbance, and governs the degree of consolidation
$\bar{\sigma}'_z$	Average effective stress in the unit cell at depth z (kPa)
$m_v _z$	Coefficient of compressibility at depth z (kPa) ⁻¹
U_z	Degree of consolidation at depth z
U	Average degree of consolidation
λ_i	Indicator function

Introduction

Constructions in soft soil deposits often require expensive solutions involving deep foundations and/or removal and replacement of the soft deposits with compacted sand layers. A less expensive, convenient, and more environment-friendly approach involves application of prefabricated vertical drains (PVDs), which are particularly useful in improving the properties of deep deposits of soft clayey soils. The PVDs, used mostly in conjunction with preloading, act as vertical drainage channels, thereby increasing the effective hydraulic conductivity of soft clays because of which consolidation in the soft deposits gets accelerated, resulting in rapid gain in shear strength and stiffness [1–6]. The PVDs are installed with a center-to-center horizontal spacing of about 1–3 m following a square or triangular pattern in plan [7, 8]. PVDs usually have a rectangular cross section with dimensions 100 mm × 4 mm, and consist of a perforated and grooved plastic core (that acts as the drainage path) encased within a woven or nonwoven filter sleeve. The aperture of filter sleeves is so chosen that the water from the soil pores can enter the PVD core easily, but the fine soil particles are prevented from entering the PVD core, and this reduces the potential for clogging [9].

PVDs are usually installed by pushing hollow steel mandrels into the ground. The bottom of the mandrel is secured by a steel anchor plate with which the PVD is attached. As the mandrel is pushed into the ground, the surrounding soil gets considerably disturbed and this results in a reduction in the hydraulic conductivity of the disturbed soil. This reduction slows down the consolidation because of which it is important to characterize the soil disturbance and incorporate its effect in the design of PVDs [3, 7, 10–14]. Apart from soil disturbance, there are other operational problems associated with PVDs, e.g., clogging of filter sleeves; reduction in PVD discharge capacity (well resistance); and bending, folding, crimping, and kinking of PVDs. However, modern manufacturing of PVDs have reduced or eliminated most of the operational problems except soil disturbance.

Several research studies have been performed on soil disturbance characterizing the extent of the disturbed zone and the degree of soil disturbance [10, 14–19]. It is generally agreed by most researchers that the disturbed zone surrounding the PVDs consists of an inner smear zone in which the soil is completely remolded and an outer transition zone in which the degree of disturbance is less compared with that in the smear zone [14, 16, 20–23]. The extent and shape of the disturbed zone and the degree of soil disturbance depend on the size and shape of mandrel, speed and type of PVD installation, and the sensitivity of the soil [23, 24]. A variety of mandrels with different cross sections (circular, rectangular or diamond shaped) are used [4, 25]. For a non-circular mandrel, the disturbed zone is likely to have a non-circular cross section. However, it is customary to convert the area of non-circular mandrels and the corresponding cross sections of the disturbed zones surrounding the PVDs to equivalent circular areas.

Analysis of PVD-aided consolidation has been performed by several researchers using analytical methods, numerical methods, and a combination of analytical and numerical methods [11, 26–29]. Based on Terzaghi's theory of one-dimensional consolidation, Barron [30] presented a comprehensive analytical solution for vertical drain-assisted consolidation of soft soils and subsequently Barron [7] modified his work to include the effect of soil disturbance. Hansbo [11] extended a study by Yoshikuni and Nakanodo [31] and produced a simple analytical solution for vertical drain consolidation considering both soil disturbance and well resistance. Basu et al. [26] and Walker and Indraratna [27] extended the work by Hansbo [11] by considering different possible spatial variations of hydraulic conductivity in the disturbed zone.

In the development of analytical solutions of PVD-aided consolidation, variations of soil properties and initial excess pore pressure with depth are largely ignored. For numerical analysis, the finite difference or finite element methods are mostly used to capture the variation of soil properties with depth [28, 32], although a few analytical and semi-analytical methods have been developed as well by considering explicit soil layering [33–35]. Laboratory-scale and field studies show that the initial excess pore pressure varies with depth [25, 36–38]. The initial excess pore pressure may vary quite significantly with depth for clay layers in which the horizontal extent of the applied vertical load (per unit area) is finite and is of the same order of magnitude as that of the clay layer thickness [39]. The exact variation of the initial excess pore pressure with depth at a site depends on the loading and drainage conditions and on the subsurface site characteristics.

However, no analytical solution exists that captures the variation of initial excess pore pressure with depth.

The objective of the present study is to develop closed-form analytical solutions for consolidation by PVDs considering the variation of initial excess pore pressure and soil properties with depth. The analytical approach of Hansbo [11] and Basu et al. [26] is extended to incorporate in the analysis the spatial variations of initial excess pore pressure and coefficient of consolidation. Closed-form solutions are developed for a few specific cases that are representative of the real field conditions. Parametric studies are performed to investigate how vertical variations of the initial excess pore pressure and coefficient of consolidation affect the PVD performance.

Analysis

Problem Definition

A PVD with a rectangular cross section of width d_w and thickness d_t is assumed to be installed in a soft clayey soil deposit consisting of p layers (Fig. 1). For analysis, it is customary to convert the rectangular cross section into an equivalent circular cross section of radius r_d by equating the perimeters of the actual and equivalent drains [11, 40]. Thus, r_d is given by

$$r_d = \frac{1}{\pi} (d_w + d_t). \tag{1}$$

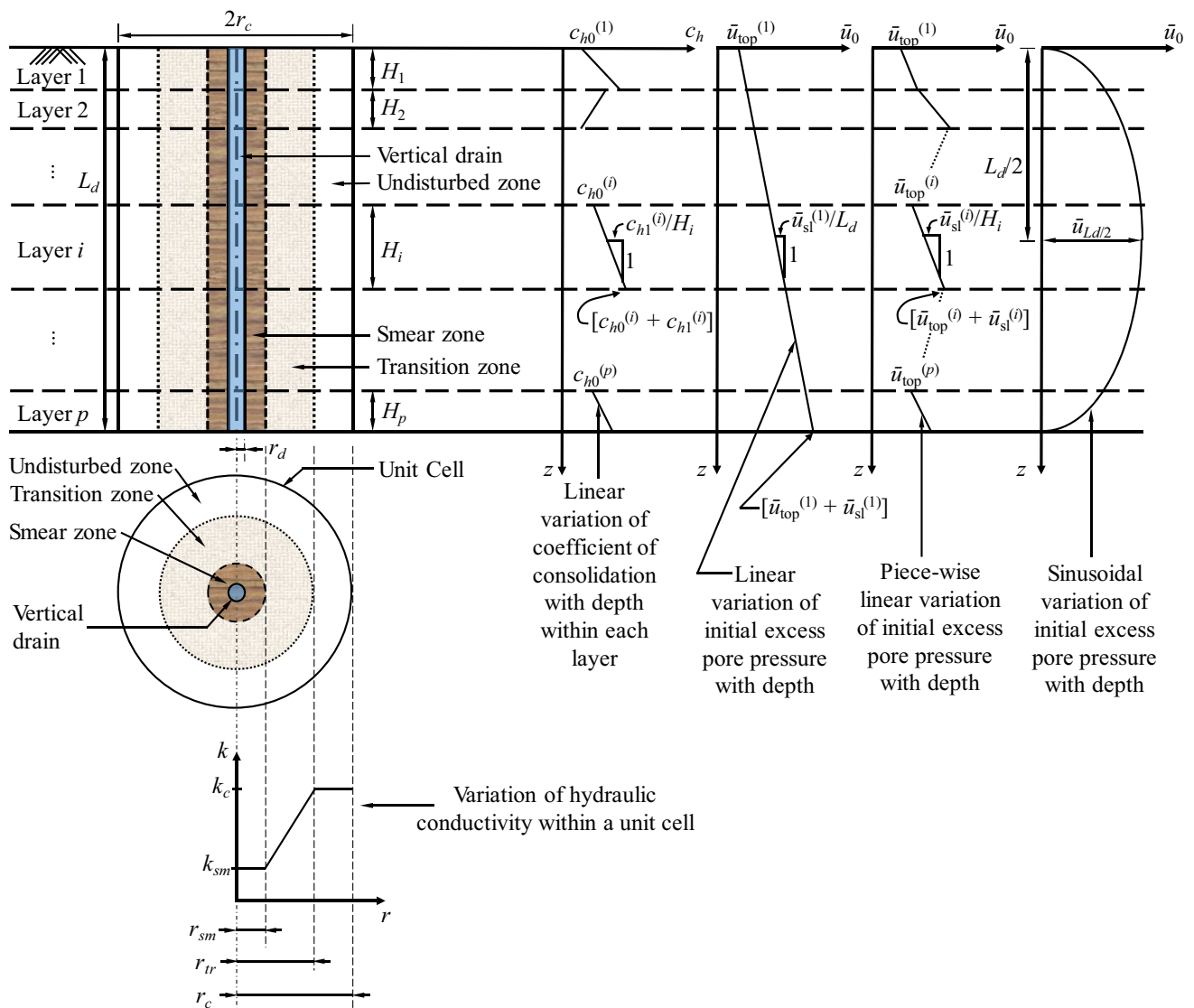


Fig. 1 Vertical drain installed in a multi-layered clayey soil with different spatial variations of initial excess pore pressure and coefficient of consolidation

For PVDs with a standard cross section of 100 mm × 4 mm, $r_d = 33.1$ mm. The length of the drain L_d spans the entire thickness of the soft soil deposit (i.e., the PVD completely penetrates the clayey deposit), which is underlain by a sand or rock layer. The thickness of any clay layer i is H_i such that $L_d = \sum_{i=1}^p H_i$. It is customary to analyze PVDs using the unit cell concept in which it is assumed that a typical PVD drains water from the surrounding soil, which is its zone of influence or unit cell, and water from one unit cell does not flow into the unit cells of adjacent PVDs (i.e., unit cells have impervious outer boundaries). For square and triangular PVD installation arrangement, the unit cell is square and hexagonal in plan, respectively. It is customary to convert these square and hexagonal unit cells into equivalent circular unit cells by equating the cross-sectional areas of the square and hexagonal unit cells with those of the equivalent circular unit cells. Therefore, in this study, a cylinder of soil with radius r_c surrounding the cylindrical drain is considered to be the unit cell (r_c is the unit cell radius) such that the vertical axes of symmetry of both the unit cell and drain coincide. For square and triangular PVD installations with center-to-center spacing s , $r_c = 0.564 s$ and $0.525 s$, respectively.

Flow of water in the vertical direction within the unit cell is neglected, as it has been found that the effect of vertical flow on PVD consolidation is not significant [41]. Moreover, as flow cannot occur across unit cells (i.e., the outer vertical boundary of the unit cell is impervious), flow of water within the unit cell can occur only horizontally following radially convergent path lines into the drain (the interface between the drain and the unit cell is the only pervious boundary). Following Hansbo [11], it is assumed that, in the unit cell, there is no horizontal strain and the vertical strain is spatially uniform within a horizontal plane (i.e., “equal-strain” consolidation is assumed). Therefore, flow is axisymmetric and flow patterns are identical along any horizontal plane. Moreover, the flow of water is assumed to follow Darcy’s law.

The in situ properties of soil like the hydraulic conductivity k , coefficient of compressibility m_v , and coefficient of consolidation c_h for flow in the horizontal direction within each layer i are assumed to vary with depth. Further, it is assumed that the initial excess pore pressure \bar{u}_0 varies with depth. A cylindrical ($r-z$) coordinate system, with r representing the radial distance (in any horizontal plane) from the center of the drain and z representing the depth from ground surface, is used in the analysis (Fig. 1).

Characterization of the Disturbed Zone

The smear and transition zones are assumed to be annular in cross section with outer radii (as measured from the

center of the drain) r_{sm} and r_{tr} , respectively (r_{sm} is the smear zone radius and r_{tr} is the transition zone radius). Soil disturbance is generally characterized in terms of soil hydraulic conductivity k (Fig. 1). The conductivity k_{sm} in the highly disturbed smear zone (i.e., for $r_d \leq r \leq r_{sm}$) is assumed to be spatially constant and is a fraction β of the conductivity k_c within the undisturbed soil [24]. The hydraulic conductivity k_c remains spatially constant in the undisturbed zone (i.e., for $r_{tr} \leq r \leq r_c$). The conductivity k_{tr} in the transition zone increases gradually from k_{sm} to k_c with an increase in the horizontal distance from the PVD [23, 24]. While the actual horizontal variation of hydraulic conductivity in the transition zone cannot be determined with certainty and different suggestions for the variation have been made [26, 27], it is reasonable to assume a linear variation (Fig. 1). Thus, in the transition zone (i.e., for $r_{sm} \leq r \leq r_{tr}$), the hydraulic conductivity $k_{tr}(r)$ increases linearly from k_{sm} at the smear zone boundary ($r = r_{sm}$) to k_c at the transition zone boundary ($r = r_{tr}$). This linear variation of $k_{tr}(r)$ in the radial direction can be expressed mathematically as

$$k_{tr}(r) = k_{sm} + \frac{r - r_{sm}}{r_{tr} - r_{sm}} (k_c - k_{sm}) \quad \text{for } r_{sm} \leq r \leq r_{tr}. \quad (2)$$

Basu and Prezzi [23, 24] showed based on an extensive review of the literature that the fraction $\beta (=k_{sm}/k_c)$ has a typical range of 0.1–0.3, the smear zone extends horizontally to a distance of 2–3 times the equivalent mandrel radius $r_{m,eq}$ [i.e., $r_{sm} = (2-3)r_{m,eq}$], and that the transition zone extends horizontally to a distance of up to about 16 times $r_{m,eq}$ (i.e., $r_{tr} \leq 16r_{m,eq}$) with the most likely range being 8–12 times $r_{m,eq}$ [i.e., $r_{tr} = (8-12)r_{m,eq}$].

Characterization of Soil Properties with Depth

Soil properties often vary with depth within a particular soil layer. An approximate way of capturing this variation is by artificially dividing the layer into multiple sublayers and then assigning different values of soil properties within each sublayer following the actual trends of variation of the properties with depth. While such an approach is acceptable for all practical purposes, it often makes the solution cumbersome and time-consuming (particularly for numerical analysis). Simpler and quicker solutions may be obtained without dividing a soil layer into sublayers when the soil properties follow simple trends like a linear variation with depth. For most clayey soil deposits, properties within a layer are either constant with depth or vary linearly. Accordingly, it is assumed in this study that soil properties vary linearly within each layer with the understanding that any other type of variation (e.g., quadratic variation) with depth can be captured by piecewise linear approximation. Such an approach reduces the required number of sublayers within each layer

from what would be required if only constant values of properties are assumed within each sublayer. At the same time, no artificial sublayering is necessary if the variation of properties with depth is indeed linear within any layer. Note that the case of spatially constant soil properties with depth is a degenerate version of the case of linear variation in which the gradient of linear variation with depth is zero.

The soil properties that are used in the derivation of the analytical solutions include the hydraulic conductivity k , coefficient of compressibility m_v , and coefficient of consolidation c_h for flow in the horizontal direction. In fact, c_h , m_v , and k_c (hydraulic conductivity in the undisturbed zone) are related by

$$c_h = \frac{k_c}{m_v \gamma_w}, \tag{3}$$

where γ_w is the unit weight of water. Because k and m_v are assumed to vary linearly with depth within any layer i , c_h can be assumed to vary linearly with depth as well within the i th layer. Thus, the variation of c_h in any layer i (except the top layer) is given by

$$c_h^{(i)}(z) = c_{h0}^{(i)} + \frac{c_{h1}^{(i)}}{H_i} [z - (H_1 + H_2 + \dots + H_{i-1})] \text{ (for } i \geq 2), \tag{4a}$$

where c_{h0} is the spatially constant part of coefficient of consolidation in any layer ($c_{h0}^{(i)}$ is the coefficient of consolidation at the top of the i th layer) and c_{h1}/H_i is the gradient with which c_h changes with depth in that layer ($c_{h0}^{(i)} + c_{h1}^{(i)}$ is the coefficient of consolidation at the bottom of the i th layer). For the top layer ($i = 1$) or for a single-layer clayey deposit ($i = 1$) with thickness $H_1 = L_d$, Eq. (4a) can be simplified to

$$c_h^{(1)}(z) = c_{h0}^{(1)} + \frac{c_{h1}^{(1)}}{H_1} z \text{ (for } i = 1). \tag{4b}$$

The time factor T representing normalized time is defined as

$$T = \frac{c_h t}{4r_c^2}, \tag{5}$$

where t is the time. As c_h is a linear function of depth within any layer, T is also a linear function of depth and, for the i th layer (except the top layer), is given by

$$T^{(i)}(z) = T_0^{(i)} + \frac{T_1^{(i)}}{H_i} [z - (H_1 + H_2 + \dots + H_{i-1})] = \frac{c_{h0}^{(i)} t}{4r_c^2} + \frac{c_{h1}^{(i)} t}{4r_c^2 H_i} \left[z - \sum_{j=1}^{i-1} H_j \right] \text{ (for } i \geq 2), \tag{6a}$$

where $T_0 [= c_{h0} t / (4r_c^2)]$ is the spatially constant part of time factor and $T_1/H_i [\text{with } T_1 = c_{h1} t / (4r_c^2)]$ is the gradient of time factor with respect to depth. For the top layer ($i = 1$) or for

a single-layer clayey deposit ($i = 1$) with thickness $H_1 = L_d$, Eq. (6a) can be simplified to

$$T^{(1)}(z) = T_0^{(1)} + \frac{T_1^{(1)}}{H_1} z = \frac{c_{h0}^{(1)} t}{4r_c^2} + \frac{c_{h1}^{(1)} t}{4r_c^2 H_1} z \text{ (for } i = 1). \tag{6b}$$

Note that, unlike the conventional approach, time factor in this formulation is different at different depths. T is a normalized time and is primarily used for generating dimensionless plots of degree of consolidation as a function of T . However, such plots cannot be developed using T as defined in Eqs. (6a) or (6b) because the time factor is no longer unique for the entire PVD–soil system, it is different for each layer and varies with depth. In this paper, for plotting the degree of consolidation as a function of normalized time, the spatially constant part of time factor $T_0^{(1)}$ of the top layer is used, unless otherwise mentioned.

Characterization of Initial Excess Pore Pressure with Depth

In conventional PVD-related consolidation analysis, it is assumed that the initial excess pore pressure \bar{u}_0 is spatially constant with depth. This is an idealized condition and is perhaps closer to reality when the clayey deposits are relatively shallow. The initial excess pore pressure is not constant with depth [15, 36–38, 42]; however, the exact variation of it with depth in PVD unit cell is not known with certainty. Finite element simulations in clayey soils suggest that there can be multiple possible variations of the initial excess pore pressure depending on the properties and thickness of the clayey deposits. Das [39] suggested different possible linear and nonlinear variations of initial excess pore pressure with depth. Accordingly, linear, piecewise linear and sinusoidal variations of initial excess pore pressure are considered in this study (Fig. 1).

For a piecewise linear variation (Fig. 1), the initial excess pore pressure in the i th layer (except the top layer) is given by

$$\bar{u}_0^{(i)}(z) = \bar{u}_{\text{top}}^{(i)} + \frac{\bar{u}_{\text{sl}}^{(i)}}{H_i} [z - (H_1 + H_2 + \dots + H_{i-1})] \text{ (for } i \geq 2), \tag{7a}$$

where $\bar{u}_{\text{top}}^{(i)}$ is the initial excess pore pressure at the top of the i th layer and $\bar{u}_{\text{sl}}^{(i)}/H_i$ is the gradient with which \bar{u}_0 changes

with depth within the i th layer ($\bar{u}_{\text{top}}^{(i)} + \bar{u}_{\text{sl}}^{(i)}$ is the initial excess pore pressure at the bottom of the i th layer). For the top layer

($i = 1$) or for a single-layer clayey deposit ($i = 1$) with thickness $H_1 = L_d$, Eq. (7a) can be rewritten as

$$\bar{u}_0^{(1)}(z) = \bar{u}_{top}^{(1)} + \frac{\bar{u}_{sl}^{(1)}}{H_1} z \text{ (for } i = 1\text{)}. \tag{7b}$$

Equation (7b) is also applicable, with H_1 replaced by L_d , for the case of multiple clay layers with a monotonically linear variation of \bar{u}_0 with depth over all the layers (Fig. 1).

For sinusoidal variation of \bar{u}_0 over the entire soft clayey deposit, the following equation can be used:

$$\bar{u}_0(z) = \bar{u}_{L_d/2} \sin\left(\frac{\pi z}{L_d}\right), \tag{8}$$

where $\bar{u}_{L_d/2}$ is the initial excess pore pressure at a depth $L_d/2$ in the soil deposit.

Average Excess Pore Pressure at Any Depth

Considering Darcy’s law and conservation of mass (i.e., continuity of flow), it can be shown that the excess pore pressures generated in the smear, transition, and undisturbed zones at any depth z within the i th layer and at any time t are given by [26]

$$u_{sm}|_z = \frac{\gamma_w}{2k_{sm,z}} \left[r_c^2 \ln\left(\frac{r}{r_d}\right) - \frac{1}{2}(r^2 - r_d^2) \right] \frac{d\varepsilon_z}{dt}, \tag{9a}$$

$$u_{tr}|_z = \frac{\gamma_w}{2} \left[\frac{r_c^2}{A} \ln\left\{ \frac{k_{sm,z} r}{(A + Br)r_{sm}} \right\} - \frac{1}{B^2} \left\{ A + Br - k_{sm,z} - A \ln\left(\frac{A + Br}{k_{sm,z}}\right) \right\} + \frac{1}{k_{sm,z}} \left\{ r_c^2 \ln\left(\frac{r_{sm}}{r_d}\right) - \frac{1}{2}(r_{sm}^2 - r_d^2) \right\} \right] \frac{d\varepsilon_z}{dt}, \tag{9b}$$

$$u_c|_z = \frac{\gamma_w}{2} \left[\frac{1}{k_{c,z}} \left\{ r_c^2 \ln\left(\frac{r}{r_{tr}}\right) - \frac{1}{2}(r^2 - r_{tr}^2) \right\} + \frac{1}{k_{sm,z}} \left\{ r_c^2 \ln\left(\frac{r_{sm}}{r_d}\right) - \frac{1}{2}(r_{sm}^2 - r_d^2) \right\} + \frac{r_c^2}{A} \ln\left(\frac{r_{tr} k_{sm,z}}{r_{sm} k_{c,z}}\right) - \frac{1}{B^2} \left\{ k_{c,z} - k_{sm,z} - A \ln\left(\frac{k_{c,z}}{k_{sm,z}}\right) \right\} \right] \frac{d\varepsilon_z}{dt}, \tag{9c}$$

where $u_{sm}|_z$, $u_{tr}|_z$, and $u_c|_z$ are the excess pore pressures in the smear, transition, and undisturbed zones, respectively, at depth z ; $k_{c,z}$ and $k_{sm,z}$ are the hydraulic conductivities of the undisturbed and smear zones, respectively, at depth z ; ε_z is the vertical strain in the unit cell at depth z and it remains spatially uniform in the horizontal plane; $A = (k_{sm,z} r_{tr} - k_{c,z} r_{sm}) / (r_{tr} - r_{sm})$, and $B = (k_{c,z} - k_{sm,z}) / (r_{tr} - r_{sm})$.

If \bar{u}_z is the average excess pore pressure in the unit cell at any depth z in the i th layer at time t , then the following

equation can be written for an annular disc of soil in the unit cell at the depth z with an infinitesimal thickness dz :

$$\int_z^{z+dz} [\pi(r_c^2 - r_d^2) \bar{u}_z] dz = \int_z^{z+dz} \left[\int_{r_d}^{r_{sm}} 2\pi r u_{sm}|_z dr + \int_{r_{sm}}^{r_{tr}} 2\pi r u_{tr}|_z dr + \int_{r_{tr}}^{r_c} 2\pi r u_c|_z dr \right] dz. \tag{10}$$

Substituting $u_{sm}|_z$, $u_{tr}|_z$, and $u_c|_z$ from Eqs. (9a, 9b, 9c) in Eq. (10), rearranging the terms, and dropping the terms with negligible contributions result in

$$\bar{u}_z = \frac{\gamma_w r_c^2}{2k_{c,z}} \frac{d\varepsilon_z}{dt} \mu_z, \tag{11}$$

where μ_z is given by

$$\mu_z = \ln\left(\frac{n}{q}\right) + \frac{1}{\beta_z} \ln(m) + \frac{(q - m)}{(\beta_z q - m)} \ln\left(\frac{\beta_z q}{m}\right) - \frac{3}{4} \tag{12}$$

with $n = r_c/r_d$, $m = r_{sm}/r_d$, $q = r_{tr}/r_d$, and $\beta_z = k_{sm,z}/k_{c,z}$. It is reasonable to assume that the disturbance caused by mandrel is uniform with depth so that the ratio of hydraulic conductivities in the smear zone and undisturbed soil at any depth remain constant, i.e., β_z is independent of depth and is equal to β , which is a constant for a PVD. Therefore, μ_z is independent of depth, is a constant for a PVD and can be

represented by μ .

Degree of Consolidation at Any Depth

Assuming that the average excess pore pressure \bar{u}_z at any depth z caused by preloading is developed instantly, the following relationship can be written:

$$\frac{d\varepsilon_z}{dt} = m_v|_z \frac{d\sigma'_z}{dt} = -m_v|_z \frac{d\bar{u}_z}{dt}, \tag{13}$$

where $\bar{\sigma}'_z$ is the average effective stress in the unit cell at depth z caused by preloading at any time, and $m_v|_z$ is the coefficient of compressibility at depth z . Substituting Eq. (11) into Eq. (13) results in the following linear differential equation:

$$\frac{d\bar{u}_z}{dt} + \frac{2k_{c,z}}{m_v|_z \gamma_w r_c^2 \mu} \bar{u}_z = 0. \tag{14}$$

Solving Eq. (14) using the initial condition that $\bar{u}_z = \bar{u}_{0z}$ at $t=0$, where \bar{u}_{0z} is the initial excess pore pressure at depth z , and using the definitions of c_h and T given by Eqs. (3, 4, 5, 6), the average excess pore pressure at depth z is obtained as function of time factor as

$$\bar{u}_z^{(i)} = \bar{u}_{0z}^{(i)} e^{-\frac{8T_z^{(i)}}{\mu}}, \tag{15}$$

where T_z is the time factor at depth z , and the superscript (i) represents the fact that the depth z lies within the i th layer.

The degree of consolidation U_z at depth z in the i th layer and at time t (or time factor T_z) is the ratio of the excess pore pressure dissipated at that depth and at that time to the initial excess pore pressure induced at that depth. U_z can be mathematically expressed as:

$$U_z = 1 - \frac{\bar{u}_z^{(i)}}{\bar{u}_{0z}^{(i)}}. \tag{16}$$

Hence, substituting Eq. (15) into Eq. (16), the degree of consolidation at any depth z within the i th layer can be obtained as

$$U_z = 1 - e^{-\frac{8T_z^{(i)}}{\mu}}. \tag{17}$$

Average Degree of Consolidation in Unit Cell

The average degree of consolidation U for the entire unit cell can be obtained by appropriately integrating the dissipated and initial excess pore pressures over all the soil layers and following a similar definition as expressed in Eq. (16). Therefore, U is given by

$$U = 1 - \frac{\int_0^{H_1} \bar{u}_z^{(1)} dz + \sum_{i=2}^p \int_{\sum_{j=1}^{i-1} H_j}^{\sum_{j=1}^i H_j} \bar{u}_z^{(i)} dz}{\int_0^{H_1} \bar{u}_{0z}^{(1)} dz + \sum_{i=2}^p \int_{\sum_{j=1}^{i-1} H_j}^{\sum_{j=1}^i H_j} \bar{u}_{0z}^{(i)} dz}. \tag{18}$$

Substituting Eq. (15) in Eq. (18), dropping the subscript z in $\bar{u}_{0z}^{(i)}$ and $T_z^{(i)}$ because average degree of consolidation U considers the initial excess pore pressure over the entire soil deposit and not just at any specific depth z , and recalling that the initial excess pore pressure \bar{u}_0 and time factor T are

functions of depth, the following equation of average degree of consolidation can be obtained:

$$U = 1 - \frac{\int_0^{H_1} \bar{u}_0^{(1)}(z) e^{-\frac{8T^{(1)}(z)}{\mu}} dz + \sum_{i=2}^p \int_{\sum_{j=1}^{i-1} H_j}^{\sum_{j=1}^i H_j} \bar{u}_0^{(i)}(z) e^{-\frac{8T^{(i)}(z)}{\mu}} dz}{\int_0^{H_1} \bar{u}_0^{(1)}(z) dz + \sum_{i=2}^p \int_{\sum_{j=1}^{i-1} H_j}^{\sum_{j=1}^i H_j} \bar{u}_0^{(i)}(z) dz}. \tag{19}$$

Specific Cases Analyzed

There are multiple possible cases with different soil layers, different variations of soil properties within each layer, and different variations of initial excess pore pressure with depth for which analytical expressions of U can be obtained. While the foregoing analysis is applicable for all such cases, obtaining explicit algebraic expressions of U for these large number of cases is beyond the scope of this study. In this paper, four specific and common cases (Cases I–IV) are considered for which close-form algebraic equations of U are determined, as described next.

Case I: Homogeneous Soil with Spatially Constant Initial Excess Pore Pressure

This is the traditional case corresponding to a soil deposit with single homogeneous clay layer in which c_h is spatially constant and the initial excess pore pressure \bar{u}_0 is spatially constant. For this case, U is given by

$$U = 1 - e^{-\frac{8T}{\mu}}, \tag{20}$$

where T is the spatially constant time factor for the problem defined by Eq. (5).

Case II: Layered Soil with Piecewise Linear Variation of Initial Excess Pore Pressure

For this case, a clayey soil deposit consisting of p layers is assumed with linear variation of c_h and linear variation of \bar{u}_0 within each layer. For this case, the variation of c_h and T with depth can be expressed by Eqs. (4a) and (6a), respectively, for $i=2, 3, \dots, p$ and by Eqs. (4b) and (6b), respectively, for $i=1$. Correspondingly, the variation of \bar{u}_0 can be expressed by Eq. (7a) for $i=2, 3, \dots, p$ and by Eq. (7b) for $i=1$. The average degree of consolidation U for this case is given by

$$U = 1 - \frac{I_N}{I_D}, \tag{21a}$$

where

$$\begin{aligned}
 I_N &= \int_0^{H_1} \left[\bar{u}_{\text{top}}^{(1)} + \frac{\bar{u}_{\text{sl}}^{(1)}}{H_1} z \right] e^{-\frac{s \left(r_0^{(1)} + \frac{r_1^{(1)}}{H_1} z \right)}{\mu}} dz + \int_{H_1}^{H_1+H_2} \left[\bar{u}_{\text{top}}^{(2)} + \frac{\bar{u}_{\text{sl}}^{(2)}}{H_2} (z - H_1) \right] e^{-\frac{s \left[r_0^{(2)} + \frac{r_1^{(2)}}{H_2} (z - H_1) \right]}{\mu}} dz \\
 &+ \dots + \int_{\sum_{i=1}^{p-1} H_i}^{\sum_{i=1}^p H_i} \left[\bar{u}_{\text{top}}^{(p)} + \frac{\bar{u}_{\text{sl}}^{(p)}}{H_2} \left(z - \sum_{i=1}^{p-1} H_i \right) \right] e^{-\frac{s \left[r_0^{(p)} + \frac{r_1^{(p)}}{H_2} \left(z - \sum_{i=1}^{p-1} H_i \right) \right]}{\mu}} dz \\
 &= \sum_{i=1}^p \left[\bar{u}_{\text{top}}^{(i)} H_i \frac{\mu}{8T_1^{(i)}} \left(e^{-\frac{sr_0^{(i)}}{\mu}} - e^{-\frac{s(r_0^{(i)}+T_1^{(i)})}{\mu}} \right) \right. \\
 &\quad \left. + \bar{u}_{\text{sl}}^{(i)} H_i \frac{\mu}{8T_1^{(i)}} \left\{ \left(\frac{\mu}{8T_1^{(i)}} \right) \left(e^{-\frac{sr_0^{(i)}}{\mu}} - e^{-\frac{s(r_0^{(i)}+T_1^{(i)})}{\mu}} \right) - e^{-\frac{s(r_0^{(i)}+T_1^{(i)})}{\mu}} \right\} \right]
 \end{aligned} \tag{21b}$$

and

$$\begin{aligned}
 I_D &= \int_0^{H_1} \left[\bar{u}_{\text{top}}^{(1)} + \frac{\bar{u}_{\text{sl}}^{(1)}}{H_1} z \right] dz + \int_{H_1}^{H_1+H_2} \left[\bar{u}_{\text{top}}^{(2)} + \frac{\bar{u}_{\text{sl}}^{(2)}}{H_2} (z - H_1) \right] dz \\
 &+ \dots + \int_{\sum_{i=1}^{p-1} H_i}^{\sum_{i=1}^p H_i} \left[\bar{u}_{\text{top}}^{(p)} + \frac{\bar{u}_{\text{sl}}^{(p)}}{H_p} \left(z - \sum_{i=1}^{p-1} H_i \right) \right] dz \\
 &= \sum_{i=1}^p \left[\bar{u}_{\text{top}}^{(i)} H_i + \frac{\bar{u}_{\text{sl}}^{(i)} H_i}{2} \right]
 \end{aligned} \tag{21c}$$

with $T_1^{(i)} \neq 0$ (i.e., when $c_{h1}^{(i)} \neq 0$). For soil profiles in which $c_{h1}^{(i)} = 0$ (i.e., c_h is constant with depth) in some of the layers (which makes $T_1^{(i)} = 0$ in those layers), I_D in Eq. (21a) is given by Eq. (21c) and I_N in Eq. (21a) is given by

$$\begin{aligned}
 I_N &= \sum_{i=1}^p \lambda_i \left[\bar{u}_{\text{top}}^{(i)} H_i \frac{\mu}{8T_1^{(i)}} \left(e^{-\frac{sr_0^{(i)}}{\mu}} - e^{-\frac{s(r_0^{(i)}+T_1^{(i)})}{\mu}} \right) \right. \\
 &\quad \left. + \bar{u}_{\text{sl}}^{(i)} H_i \frac{\mu}{8T_1^{(i)}} \left\{ \left(\frac{\mu}{8T_1^{(i)}} \right) \left(e^{-\frac{sr_0^{(i)}}{\mu}} - e^{-\frac{s(r_0^{(i)}+T_1^{(i)})}{\mu}} \right) - e^{-\frac{s(r_0^{(i)}+T_1^{(i)})}{\mu}} \right\} \right] \\
 &\quad + \sum_{i=1}^p (1 - \lambda_i) e^{-\frac{sr_0^{(i)}}{\mu}} \left[\bar{u}_{\text{top}}^{(i)} H_i + \frac{\bar{u}_{\text{sl}}^{(i)} H_i}{2} \right],
 \end{aligned} \tag{21d}$$

where the indicator function λ_i is given by

$$\lambda_i = \begin{cases} 1 & \text{if } T_1^{(i)} \neq 0 \\ 0 & \text{otherwise} \end{cases} \tag{21e}$$

Note that Eqs. are valid for problems with two or more clay layers, i.e., for $i > 1$. For the single-layer problem with $i = 1$, the solution is given in Case III (described next).

Case III: Single-Layer Soil with Linear Variation of Initial Excess Pore Pressure

For this case, a single layer of clayey soil deposit is assumed ($i = 1$) with linear variation of c_h and linear variation of \bar{u}_0 . The variation of c_h and T with depth can be expressed by Eqs. (4b) and (6b), respectively, with $H_1 = L_d$. Correspondingly, the variation of \bar{u}_0 can be expressed by Eq. (7b) with H_1 replaced by L_d . Thus, U for this case is given by

$$\begin{aligned}
 U &= 1 - \frac{\int_0^{L_d} \left[\bar{u}_{\text{top}}^{(1)} + \frac{\bar{u}_{\text{sl}}^{(1)}}{L_d} z \right] e^{-\frac{8\left(\tau_0^{(1)} + \tau_1^{(1)}\right)z}{\mu}} dz}{\int_0^{L_d} \left[\bar{u}_{\text{top}}^{(1)} + \frac{\bar{u}_{\text{sl}}^{(1)}}{L_d} z \right] dz} \\
 &= 1 - \frac{\frac{\mu}{8T_1^{(1)}} \left(e^{-\frac{8\tau_0^{(1)}}{\mu}} - e^{-\frac{8\left(\tau_0^{(1)} + \tau_1^{(1)}\right)}{\mu}} \right) + \frac{\bar{u}_{\text{sl}}^{(1)}}{\bar{u}_{\text{top}}^{(1)}} \frac{\mu}{8T_1^{(1)}} \left[\left(\frac{\mu}{8T_1^{(1)}} \right) \left(e^{-\frac{8\tau_0^{(1)}}{\mu}} - e^{-\frac{8\left(\tau_0^{(1)} + \tau_1^{(1)}\right)}{\mu}} \right) - e^{-\frac{8\left(\tau_0^{(1)} + \tau_1^{(1)}\right)}{\mu}} \right]}{1 + \frac{\bar{u}_{\text{sl}}^{(1)}}{2\bar{u}_{\text{top}}^{(1)}}}
 \end{aligned} \tag{22a}$$

with $T_1^{(1)} \neq 0$ (i.e., when $c_{h1}^{(1)} \neq 0$). For the particular case of $c_{h1}^{(1)} = 0$ (i.e., when c_h is constant with depth) that makes $T_1^{(1)} = 0$, U is given by Eq. (20). Further, for the special case of spatially constant \bar{u}_0 in a single-layer clay deposit with linearly varying c_h , U is given by

$$U = 1 - \frac{\mu}{8T_1^{(1)}} \left(e^{-\frac{8\tau_0^{(1)}}{\mu}} - e^{-\frac{8\left(\tau_0^{(1)} + \tau_1^{(1)}\right)}{\mu}} \right). \tag{22b}$$

Case IV: Single-Layer Soil with Sinusoidal Variation of Initial Excess Pore Pressure

For this case, a clayey deposit consisting of a single layer is assumed with linear variation of c_h and sinusoidal variation of \bar{u}_0 . Therefore, the variation of c_h and T with depth can be expressed by Eqs. (4b) and (6b), respectively, with $H_1 = L_d$. The variation of \bar{u}_0 can be expressed using Eq. (8). The average degree of consolidation U for this case is given by

$$\begin{aligned}
 U &= 1 - \frac{\int_0^{L_d} \bar{u}_{L_d/2} \sin\left(\frac{\pi z}{L_d}\right) e^{-\frac{8\left(\tau_0^{(1)} + \tau_1^{(1)}\right)z}{\mu}} dz}{\int_0^{L_d} \bar{u}_{L_d/2} \sin\left(\frac{\pi z}{L_d}\right) dz} \\
 &= 1 - \frac{\left(\frac{\pi\mu}{8T_1^{(1)}}\right)^2 \left[e^{-\frac{8\left(\tau_0^{(1)} + \tau_1^{(1)}\right)}{\mu}} + e^{-\frac{8\tau_0^{(1)}}{\mu}} \right]}{1 + \left(\frac{\pi\mu}{8T_1^{(1)}}\right)^2}
 \end{aligned} \tag{23}$$

with $T_1^{(1)} \neq 0$ (i.e., when $c_{h1}^{(1)} \neq 0$). Note that U is independent of the value of initial excess pore pressure $\bar{u}_{L_d/2}$ at the center of the clay layer. For the particular case of $c_{h1}^{(1)} = 0$ (i.e., when c_h is constant with depth) that makes $T_1^{(1)} = 0$, U is given by Eq. (20).

It is evident from the foregoing equations that, for single-layer, homogeneous clay deposits with spatially constant c_h , the different spatial variations of initial excess pore pressure

produce the same rate of consolidation. However, soil properties vary with depth in almost every site because of which the foregoing closed-form solutions have practical relevance.

Validation

Lim et al. [43] reported a field study on PVDs in which the pore pressure and coefficient of consolidation varied with depth. PVDs with cross-sectional dimensions 100 mm × 3 mm were installed with a rectangular mandrel of dimensions 120 mm × 60 mm at a site comprising 10.5 m-thick soft Ballina clay in a square arrangement with a center-to-center spacing of 1.2 m. Based on the data presented by Lim et al. [43], c_h at the site varies from 147 m²/year at the ground surface to about 3 m²/year at the bottom of the layer, and \bar{u}_0 varies from 40 kPa at the ground surface

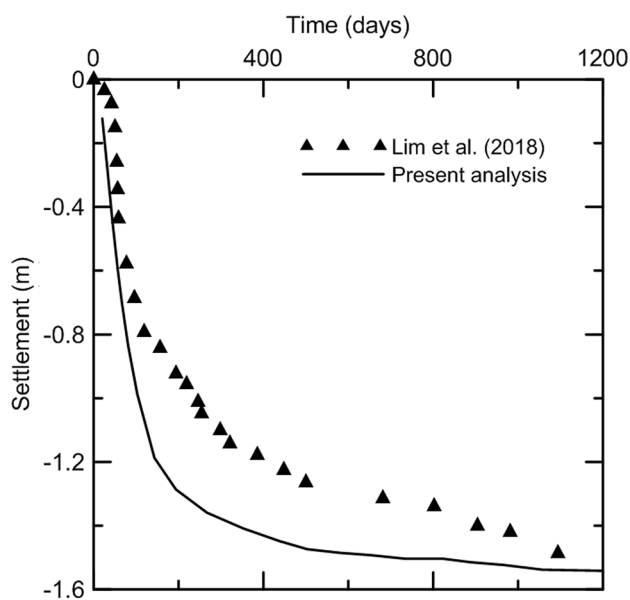


Fig. 2 Comparison of settlement versus time response at a Ballina clay site improved with PVDs obtained from the present analysis and field measurements

to 145 kPa at the bottom of the layer. The authors did not mention about the specifics of soil disturbance, but from the discussion presented $\beta=0.5$ can be assumed. Using the equation of μ proposed by Hansbo [11], which was used by Lim et al. [43], a value of $\mu=3.5$ is obtained. The settlement versus time plots obtained from field measurements are provided by Lim et al. [43]. The field response of the PVDs is simulated using the present analysis, and it is assumed that the degree of consolidation U at any time t is the ratio of the surface settlement at that time to the ultimate surface settlement. The time versus settlement plots obtained from the present analysis and measured in the field are shown in Fig. 2, and a reasonably good match is obtained. This shows that the developed analytical solutions are applicable in the field.

Parametric Study

Parametric studies are performed to investigate the effect of spatial variation of c_h and \bar{u}_0 on the rate of PVD consolidation. While performing these studies, the degree of soil disturbance and the extent of the disturbed zone are kept constants to focus only on c_h and \bar{u}_0 , and their variations. The degree of disturbance characterized by β is assumed to be 0.2 for all the problems. Similarly, for all the problems, the radius of smear zone r_{sm} is assumed to be $2r_{m,eq}$ and the radius of the transition zone r_{tr} is assumed to be $10r_{m,eq}$. A mandrel cross section of 125 mm \times 50 mm is assumed for all the problems, which yields $r_{m,eq} = \sqrt{(125 \times 50)/\pi} = 44.6$ mm,

so that $r_{sm} = 89.2$ mm and $r_{tr} = 446.0$ mm. Thus, for the problems that follow, $m = r_{sm}/r_d = 89.2/33.1 = 2.69$ and $q = r_{tr}/r_d = 446/33.1 = 13.47$. Further, a square PVD arrangement is assumed with spacing $s = 1.0$ m, 2.0 m, and 3.0 m, which results in unit cell radius $r_c = 0.564$ m, 1.128 m, and 1.692 m, and $n (= r_c/r_d) = 17.04, 34.08,$ and 51.12, respectively. Therefore, the values of μ used in this study are 9.83, 10.52, and 10.93 for PVD spacing $s = 1$ m, 2 m, and 3 m, respectively.

Effect of Spatial Variation of Soil Properties

To investigate the impact of spatial variation of c_h on the degree of consolidation U , a single-layer problem is considered with spatially constant \bar{u}_0 (i.e., $\bar{u}_{sl}^{(1)}/\bar{u}_{top}^{(1)} = 0$), but with c_h varying linearly with depth ($c_{h1}^{(1)}/c_{h0}^{(1)} \neq 0$). The single clay layer is assumed to be 10-m thick ($L_d = H_1 = 10$ m). The PVDs are assumed to be installed with a square arrangement with center-to-center spacing $s = 1$ m (i.e., $r_c = 0.564$ m). Figure 3 shows the variation of U as a function of $T_0^{(1)}$ for different values of $c_{h1}^{(1)}/c_{h0}^{(1)}$ ($= -0.5, 0, 0.5, 1.0,$ and 2.0). It is evident that soil deposits get consolidated faster with an increase in $c_{h1}^{(1)}/c_{h0}^{(1)}$. Further, the effect of decrease of c_h with depth on the consolidation rate is more pronounced than the effect of increase of c_h with depth.

Figure 4 shows the U versus T plots for a 10-m-thick single clay layer ($L_d = H_1 = 10$ m) with $r_c = 0.564$ m (i.e., 1-m

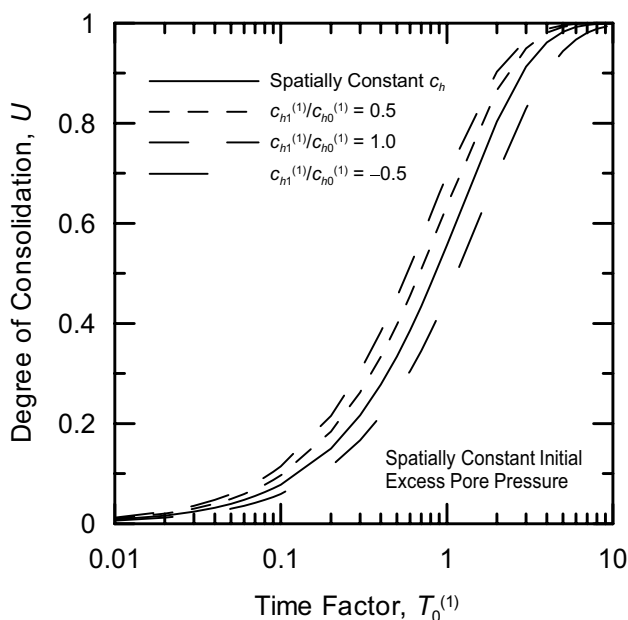


Fig. 3 Effect of spatially varying coefficient of consolidation on the consolidation rate in 10-m-thick clay deposits

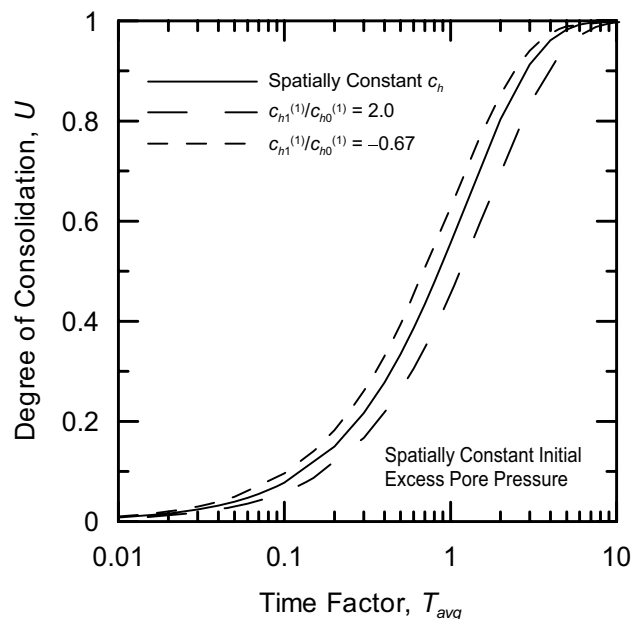


Fig. 4 Degree of consolidation as a function of average time factor for spatially constant, linearly increasing, and linearly decreasing coefficient of consolidation in 10-m-thick clay deposits with the same average coefficient of consolidation

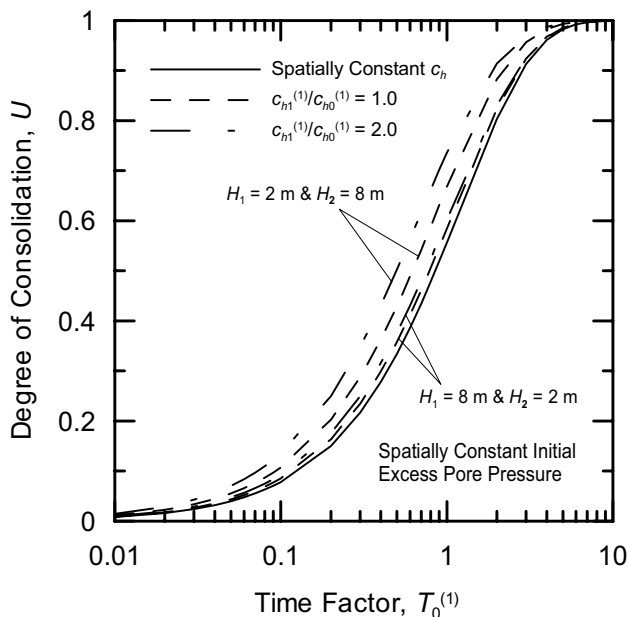


Fig. 5 Effect of soil layering on the rate of consolidation for 10-m-thick two-layer clay deposits

center-to-center PVD spacing with square arrangement) and spatially constant \bar{u}_0 (i.e., $\bar{u}_{sl}^{(1)}/\bar{u}_{top}^{(1)} = 0$) with three different variations of c_h : (1) a spatially constant coefficient of consolidation = $c_{h,avg}$ ($= 5 \text{ m}^2/\text{year}$, say); (2) a linearly increasing coefficient of consolidation with $c_{h0}^{(1)} = c_{h,avg}/2$ ($= 2.5 \text{ m}^2/\text{year}$, say) at the ground surface, $c_{h1}^{(1)}/c_{h0}^{(1)} = 2.0$, and $c_{h0}^{(1)} + c_{h1}^{(1)} = 3c_{h,avg}/2$ ($= 7.5 \text{ m}^2/\text{year}$, say) at 10-m depth; and (3) a linearly decreasing coefficient of consolidation with $c_{h0}^{(1)} = 3c_{h,avg}/2$ ($= 7.5 \text{ m}^2/\text{year}$, say) at the ground surface, $c_{h1}^{(1)}/c_{h0}^{(1)} = -(2/3)$, and $c_{h0}^{(1)} + c_{h1}^{(1)} = c_{h,avg}/2$ ($= 2.5 \text{ m}^2/\text{year}$, say) at 10-m depth. Note that the average coefficient of consolidation for the three variations of c_h is $c_{h,avg}$. Figure 4 shows the U versus T plots in which T_{avg} ($= c_{h,avg} t/r_c^2$) is used to obtain the plots. The figure shows that, for spatially varying soil properties, the assumption of a constant average degree of consolidation may lead to erroneous results with the error being more for the spatially increasing case.

Figure 5 shows the U versus $T_0^{(1)}$ plots for PVDs installed in a square arrangement with a spacing of 1 m ($r_c = 0.564 \text{ m}$) in a 10-m-thick clay deposit consisting of two layers ($L_d = H_1 + H_2 = 10 \text{ m}$) with spatially constant \bar{u}_0 (i.e., $\bar{u}_{top}^{(1)} = \bar{u}_{top}^{(2)}$ and $\bar{u}_{sl}^{(1)} = \bar{u}_{sl}^{(2)} = 0 \text{ kPa}$). For this problem, c_h is assumed to be spatially constant in the top layer but increases linearly in the second layer from the constant value of the top layer (i.e., $c_{h1}^{(1)}/c_{h0}^{(1)} = 0$, $c_{h0}^{(2)} = c_{h0}^{(1)}$, and $c_{h1}^{(2)}/c_{h0}^{(2)} \neq 0$). It is evident that if the second layer covers a large part of the PVD (as in the case with $H_1 = 2 \text{ m}$ and $H_2 = 8 \text{ m}$), then the spatial variation of c_h in the second layer

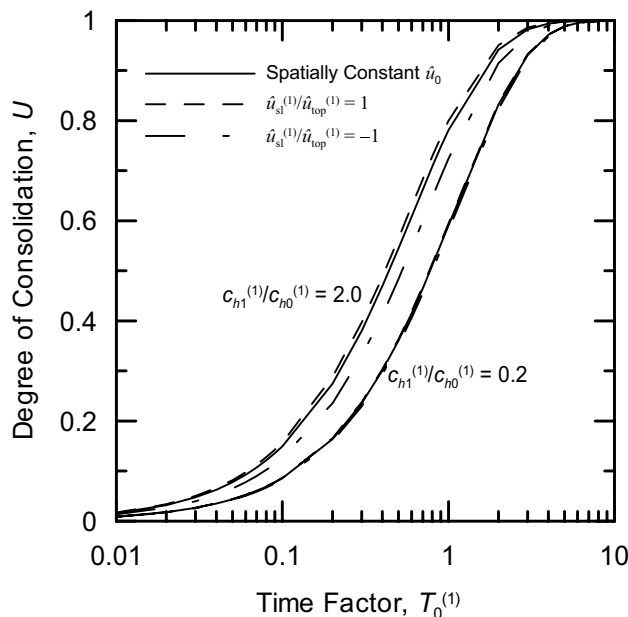


Fig. 6 Effect of spatially varying initial excess pore pressure on the rate of consolidation in 10-m-thick clay deposits

has a substantial impact on the rate of consolidation. If the second layer covers only a small part of the PVD (as in the case with $H_1 = 8 \text{ m}$ and $H_2 = 2 \text{ m}$), then the effect of spatial variation of c_h in the second layer on the rate of consolidation is rather modest.

Effect of Spatial Variation of Initial Excess Pore Pressure

Figure 6 shows the effect of spatial variation of \bar{u}_0 on the consolidation rate for linearly varying \bar{u}_0 in a 10-m-thick single-layer clay deposit ($L_d = H_1 = 10 \text{ m}$) with $r_c = 0.564 \text{ m}$ (i.e., PVD is installed in a square arrangement with $s = 1 \text{ m}$). For this figure, three different variations are considered in which (1) \bar{u}_0 is assumed to be spatially constant at 100 kPa (i.e., $\bar{u}_{top}^{(1)} = 100 \text{ kPa}$ and $\bar{u}_{sl}^{(1)}/\bar{u}_{top}^{(1)} = 0$); (2) \bar{u}_0 increases linearly from 100 kPa at the ground surface to 200 kPa at $z = 10 \text{ m}$ ($\bar{u}_{top}^{(1)} = 100 \text{ kPa}$ and $\bar{u}_{sl}^{(1)}/\bar{u}_{top}^{(1)} = 1$); and (3) \bar{u}_0 decreases linearly from 100 kPa at the ground surface to 0 kPa at $z = 10 \text{ m}$ at $z = 10 \text{ m}$ ($\bar{u}_{top}^{(1)} = 100 \text{ kPa}$ and $\bar{u}_{sl}^{(1)}/\bar{u}_{top}^{(1)} = -1$). The U versus $T_0^{(1)}$ plots for these three variations of \bar{u}_0 are shown in Fig. 6 for $c_{h1}^{(1)}/c_{h0}^{(1)} = 0.2$ and 2.0. Linear decrease in \bar{u}_0 with depth results in slower consolidation than compared with the case with linear increase of \bar{u}_0 with depth or with spatially constant \bar{u}_0 . Further, when \bar{u}_0 increases with depth, consolidation occurs faster than when

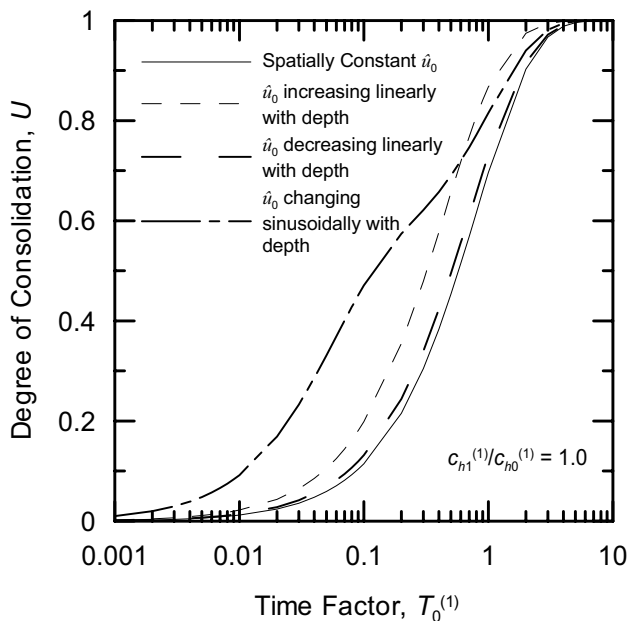


Fig. 7 Degree of consolidation for different spatial variations of initial excess pore pressure \bar{u}_0 in a 10-m-thick clay layer such that $\bar{u}_0 = 100$ kPa at the center of the clay layer

\bar{u}_0 is constant with depth. However, the change in consolidation rate because of change in the spatial variation of \bar{u}_0 is much less compared with that because of change in spatial variation of c_h .

Figure 7 shows the U versus $T_0^{(1)}$ plots for four different variations of \bar{u}_0 with depth in a 10-m-thick clay deposit ($L_d = H_1 = 10$ m) with $r_c = 0.564$ m such that $\bar{u}_0 = 100$ kPa at the center of the clay deposit (i.e., at $z = 5$ m). The variations assumed are as follows: (1) \bar{u}_0 is spatially constant at 100 kPa (i.e., $\bar{u}_{top}^{(1)} = 100$ kPa and $\bar{u}_{sl}^{(1)}/\bar{u}_{top}^{(1)} = 0$); (2) \bar{u}_0 varies linearly from 0 kPa at the ground surface to 200 kPa at $z = 10$ m (i.e., $\bar{u}_{top}^{(1)} = 0$ kPa and $\bar{u}_{sl}^{(1)} = 200$ kPa); (3) \bar{u}_0 varies linearly from 200 kPa at the ground surface to 0 kPa at $z = 10$ m (i.e., $\bar{u}_{top}^{(1)} = 200$ kPa and $\bar{u}_{sl}^{(1)} = -200$ kPa); and (4) \bar{u}_0 varies sinusoidally with depth following Eq. (8). The ratio $c_{h1}^{(1)}/c_{h0}^{(1)}$ is maintained at 1.0 for these plots. It is clear that sinusoidal variation of \bar{u}_0 results in a very different U versus T plot than those corresponding to monotonic linear variation of \bar{u}_0 . Further, using a spatially constant \bar{u}_0 with an average value in place of the actual variation of \bar{u}_0 may not produce accurate results, as is clear from a comparison of the plots corresponding to the linearly increasing, linearly decreasing, and spatially constant \bar{u}_0 .

Effect of Clay Layer Thickness and PVD Spacing

To investigate the effect of thickness L_d of the soft deposit on the rate of consolidation, three single-layer clay deposits

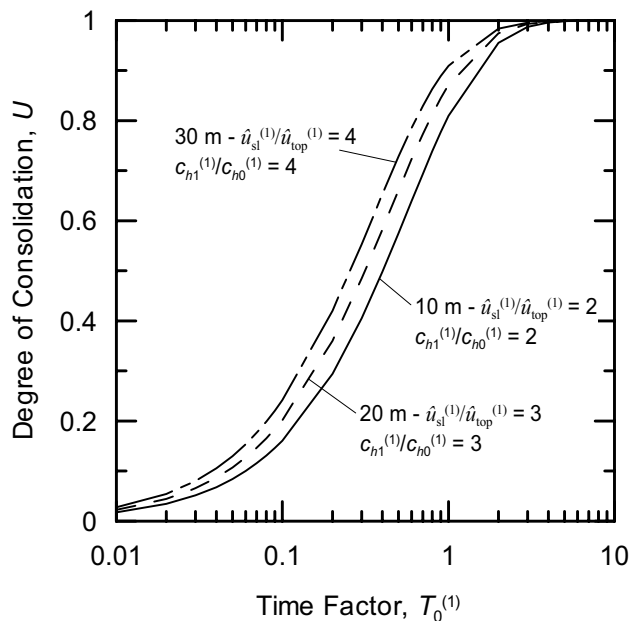


Fig. 8 Degree of consolidation versus time factor plots for 10-m, 20-m, and 30-m-thick clay deposits with $c_{h1}^{(1)}/L_d = 0.1$ m/year and $\bar{u}_{sl}^{(1)}/L_d = 10$ kPa/m

are considered with $L_d (= H_1) = 10$ m, 20 m, and 30 m and with linear variations of c_h and \bar{u}_0 in the deposits. Square PVD arrangement with spacing $s = 1$ m is assumed ($r_c = 0.564$ m). In these three deposits, c_h varies from 1 m²/year at the ground surface (i.e., $c_{h0}^{(1)} = 1$ m²/year) to 2 m²/year, 3 m²/year, and 4 m²/year at depths of 10 m, 20 m, and 30 m, respectively, such that $c_{h1}^{(1)}/L_d = 0.1$ m/year in all the three clay deposits. Thus, $c_{h1}^{(1)}/c_{h0}^{(1)} = 2, 3,$ and 4 for 10 m, 20 m, and 30 m, respectively. For these deposits, the initial excess pore pressure varies from 100 kPa at the ground surface (i.e., $\bar{u}_{top}^{(1)} = 100$ kPa) to 200 kPa, 300 kPa, and 400 kPa at depths of 10 m, 20 m, and 30 m (i.e., $\bar{u}_{sl}^{(1)} = 100$ kPa, $\bar{u}_{sl}^{(1)} = 200$ kPa, and $\bar{u}_{sl}^{(1)} = 300$ kPa for $L_d = 10$ m, 20 m, and 30 m, respectively). Note that $\bar{u}_{sl}^{(1)}/L_d = 10$ kPa/m for all the three soil deposits. Figure 8 shows the U versus $T_0^{(1)}$ plots. As c_h and \bar{u}_0 increase with depth creating a favorable condition for faster flow, the rate of consolidation is the maximum for the 30-m-thick layer and decreases with a decrease in the thickness of the clay deposit.

The same set of problems with three single-layer soil deposits with $L_d (= H_1) = 10$ m, 20 m, and 30 m, and $r_c = 0.564$ m (i.e., $s = 1$ m with a square arrangement) are reanalyzed with changed values of c_h and \bar{u}_0 at the base of the clay layers. For this set of problems, c_h varies from 1 m²/year at the ground surface (i.e., $c_{h0}^{(1)} = 1$ m²/year) to 2 m²/year at $z = L_d$ (i.e., $c_{h1}^{(1)} = 1$ m²/year) and the initial excess pore pressure varies from 100 kPa at the ground surface ($\bar{u}_{top}^{(1)} = 100$ kPa) to 200 kPa at $z = L_d$ for the three deposits

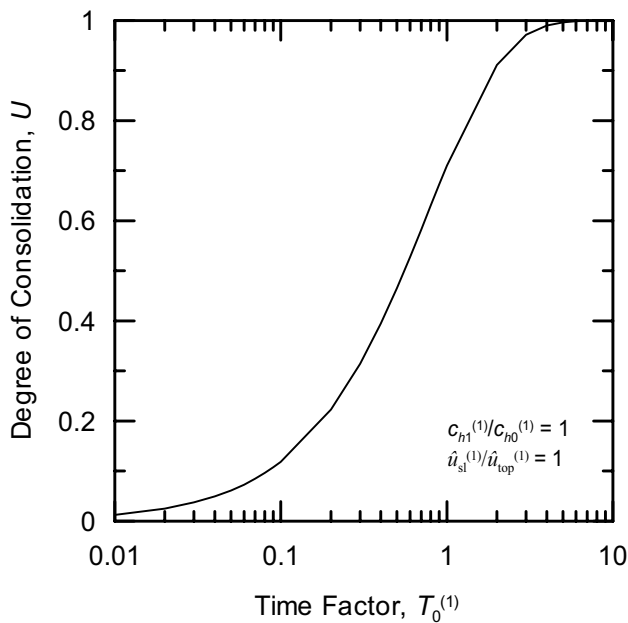


Fig. 9 Degree of consolidation versus time factor plots for 10-m, 20-m, and 30-m-thick clay deposits with $c_{h1}^{(1)}/c_{h0}^{(1)}=1.0$ and $\bar{u}_{sl}^{(1)}/\bar{u}_{top}^{(1)}=1.0$ and with a PVD spacing $s=1$ m (square arrangement)

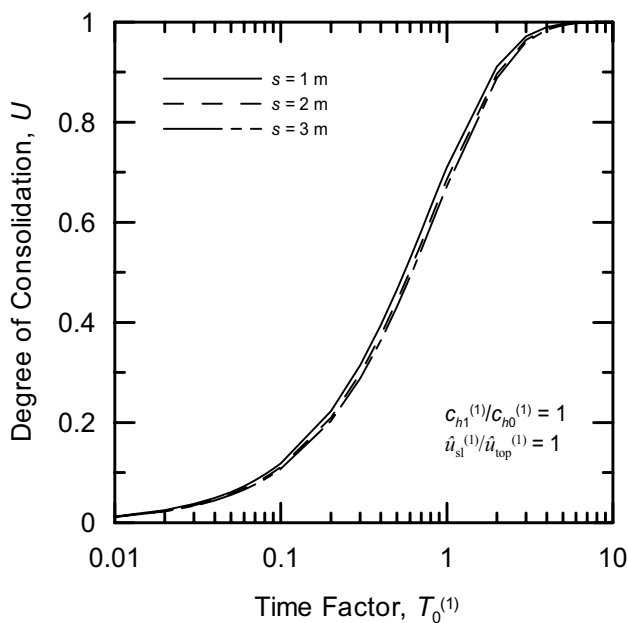


Fig. 10 Degree of consolidation versus time factor plots for 10-m, 20-m, and 30-m-thick clay deposits with $c_{h1}^{(1)}/c_{h0}^{(1)}=1.0$ and $\bar{u}_{sl}^{(1)}/\bar{u}_{top}^{(1)}=1.0$, and with PVD spacings $s=1$ m, 2 m, and 3 m (square arrangement)

($\bar{u}_{sl}^{(1)} = 100$ kPa). Thus, $c_{h1}^{(1)}/c_{h0}^{(1)}$ and $\bar{u}_{sl}^{(1)}/\bar{u}_{top}^{(1)}$ are maintained constants at a value of 1.0. Further, $c_{h1}^{(1)}/L_d=0.1$ m/year, 0.05 m/year, and 0.033 m/year, and $u_{sl}^{(1)}/L_d=10$ kPa/m,

5 kPa/m, and 3.33 kPa/m for the 10 m-, 20 m-, and 30-m-thick clay layers, respectively. It is interesting to note that U versus $T_0^{(1)}$ plots for the three deposits are identical and fall on top each other (Fig. 9). Thus, different single-layer soil deposits that have the same $c_{h1}^{(1)}/c_{h0}^{(1)}$ and $\bar{u}_{sl}^{(1)}/\bar{u}_{top}^{(1)}$ generate the same rate of consolidation. This was verified by choosing different sets of values for $c_{h1}^{(1)}/c_{h0}^{(1)}$ and $\bar{u}_{sl}^{(1)}/\bar{u}_{top}^{(1)}$ for the three clay deposits considered. Therefore, these ratios can be used to develop design charts.

Maintaining both $c_{h1}^{(1)}/c_{h0}^{(1)}$ and $\bar{u}_{sl}^{(1)}/\bar{u}_{top}^{(1)}$ as a constant equal to 1.0, the same 10-m-, 20-m-, and 30-m-thick single-layer clay problem is studied with different PVD spacings $s=1$ m, 2 m, and 3 m with a square arrangement (i.e., $r_c=0.564$ m, 1.128 m, and 1.692 m). The U versus $T_0^{(1)}$ plots (Fig. 10) for the different thicknesses of clay deposits are identical, but the plots corresponding to different PVD spacings are different. However, the difference between the plots is not significant. For example, the time factor T_{90} corresponding to 90% consolidation (i.e., $U=0.9$) differs by less than 3% for the three PVD spacings considered. Therefore, different single-layer soil deposits that have the same constant values of $c_{h1}^{(1)}/c_{h0}^{(1)}$ and $\bar{u}_{sl}^{(1)}/\bar{u}_{top}^{(1)}$ produce nearly identical U versus $T_0^{(1)}$ plots.

Numerical Example

The use of the analytical solutions developed in this paper is demonstrated here with the help of a practical numerical example. A 12-m-thick saturated soft clayey deposit with the water table at the ground surface is considered in which fully penetrating 100 mm × 4 mm PVDs ($r_d=33.1$ mm) are installed in triangular arrangement with a center-to-center spacing $s=1.2$ m. The drains are installed with a mandrel of cross section 150 mm × 50 mm. Circular oil tanks are to be placed on the ground that would generate a distributed vertical load of 170 kN/m² on the ground surface. In situ and laboratory measurements suggest that the coefficient of consolidation is 2.6 m²/year at the ground level and 0.8 m²/year at the base of the deposit (at a depth of 12 m). Preloading was done and the pore pressure measurements suggest that the initial excess pore pressure developed is 110 kPa at the ground surface and 30 kPa at the base of the deposit. It is required to find out how long the preloading should be kept to achieve 90% consolidation.

First, the unit cell dimension and degree of disturbance have to be quantified. It is reasonable to assume, in the absence of data, that the degree of disturbance in the smear zone $\beta=0.2$, the radius of smear zone $r_{sm}=2r_{m,eq}$ and the radius of transition zone $r_{tr}=10r_{m,eq}$. For the 150 mm × 50 mm mandrel used,

$r_{m,eq} = \sqrt{(150 \times 50)/\pi} = 48.9$ mm, so that $r_{sm} = 97.8$ mm and $r_{tr} = 489.0$ mm. Thus, $m = r_{sm}/r_d = 97.8/33.1 = 2.9547$, and $q = r_{tr}/r_d = 489/33.1 = 14.7734$. For a triangular PVD arrangement with $s = 1.2$ m, the unit cell radius $r_c = 0.525 \times 1.2 = 0.63$ m, and $n = r_c/r_d = 630/33.1 = 19.0332$. Therefore, $\mu = \ln\left(\frac{n}{q}\right) + \frac{1}{\beta} \ln(m) + \frac{(q-m)}{(\beta q-m)} \ln\left(\frac{\beta q}{m}\right) - \frac{3}{4}$
 $= \ln\left(\frac{19.0332}{14.7734}\right) + \frac{1}{0.2} \ln(2.9547) + \frac{(14.7734-2.9547)}{(0.2 \times 14.7734 - 2.9547)} \ln\left(\frac{0.2 \times 14.7734}{2.9547}\right) - \frac{3}{4} = 10.83$.

With the information on c_h and \bar{u}_0 given, it is reasonable to assume that these quantities vary linearly with depth with $c_{h0}^{(1)} = 2.6$ m²/year and $c_{h0}^{(1)} + c_{h1}^{(1)} = 0.8$ m²/year, and $\bar{u}_{top}^{(1)} = 110$ kPa and $\bar{u}_{top}^{(1)} + \bar{u}_{sl}^{(1)} = 30$ kPa. Therefore, $c_{h1}^{(1)} = 0.8 - 2.6 = -1.8$ m²/year and $\bar{u}_{sl}^{(1)} = 30 - 110 = -80$ kPa. For the depth $H_1 = 12$ m, the gradients of c_h and \bar{u}_0 are -0.15 m/year and -6.67 kPa/m. The time factor terms for this problem are given by $T_0^{(1)} = \frac{c_{h0}^{(1)} t}{4r^2} = \frac{2.6t}{4 \times 0.63^2} = 1.638t$ and $T_1^{(1)} = \frac{c_{h1}^{(1)} t}{4r^2} = -\frac{1.8t}{4 \times 0.63^2} = -1.134t$.

For linear variations of c_h and \bar{u}_0 , degree of consolidation U is given by Eq. (22a). Therefore, substituting all the calculated values, U for this problem is given by

$$U = 1 - \frac{1}{1 + \frac{-80}{2 \times 110}} \left[\frac{10.83}{8 \times (-1.134t)} \left(e^{-\frac{8 \times 1.638t}{10.83}} - e^{-\frac{8 \times (1.638t - 1.134t)}{8.83}} \right) + \frac{-80}{110} \times \frac{10.83}{8 \times (-1.134t)} \left\{ \left(\frac{10.83}{8 \times (-1.134t)} \right) \left(e^{-\frac{8 \times 1.638t}{10.83}} - e^{-\frac{8 \times (1.638t - 1.134t)}{10.83}} \right) - e^{-\frac{8 \times (1.638t - 1.134t)}{10.83}} \right\} \right]$$

Solving for $U = 0.9$ yields $t = 3.3$ years. The calculation is most conveniently done in a spreadsheet program. Note that if spatially average $c_h (= 1.7$ m²/year) and \bar{u}_0 were assumed, then Eq. (20) would be used and the estimated time $t = 2.9$ years corresponding to $U = 0.9$ would be obtained erroneously.

Conclusions

Analytical solutions are developed for radial consolidation by prefabricated vertical drains in which spatial variations of coefficient of consolidation and initial excess pore pressure are considered. A cylindrical unit cell with a cylindrical drain is assumed for the analysis after converting the rectangular shape of PVD cross section and the square or hexagonal shape of unit cell into equivalent circular shapes. Soil disturbance is also considered in the analysis with a highly disturbed inner smear zone and a less disturbed outer transition zone surrounding the PVD. The hydraulic conductivity is assumed to be a fraction of the in situ hydraulic conductivity in the smear zone and it remains spatially constant in the smear zone. The hydraulic conductivity increases linearly in the transition zone with an increase in the radial distance

from the PVD, and becomes equal to the in situ value in the undisturbed zone. Equal-strain consolidation is assumed along with Darcy’s law for flow through soil, and analytical equations for the degree of consolidation are obtained for linear and piecewise linear variations of coefficient of consolidation with depth and for linear and sinusoidal variations of initial excess pore pressure with depth. However, the theory developed in this study can be applied to multiple possible cases with different soil layers, different variations of soil properties within each layer, and different variations of initial excess pore pressure. A numerical example is provided that demonstrate the step by step calculations using the developed analytical solutions.

Parametric studies are performed to investigate the effect of spatial variations of coefficient of consolidation c_h and initial excess pore pressure \bar{u}_0 on the rate of consolidation. It is observed that the spatial variation of c_h has a strong impact on the rate of consolidation, while the spatial variation of \bar{u}_0 has a lesser impact. Different spatial variations of \bar{u}_0 , e.g., linear and sinusoidal variations, lead to different rates of consolidation if c_h varies with depth. However, for single-layer deposits with spatially constant c_h , different spa-

tial variations of \bar{u}_0 results in the same rate of consolidation. Soil layering, with different spatial variations of c_h in the different layers, has an impact on the rate of consolidation. It is observed that the ratios $c_{h1}^{(1)}/c_{h0}^{(1)}$ and $\bar{u}_{sl}^{(1)}/\bar{u}_{top}^{(1)}$ are the most important parameters for PVD-enhanced consolidation in soil deposits with spatially varying properties and spatially varying initial excess pore pressure. If these ratios are constants for different soil deposits, then the rate of consolidation is the same in these deposits irrespective of their individual properties. In fact, different spacings of PVDs also have a minimal impact on the degree of consolidation versus time factor plots of different clay deposits if these deposits have the same constant values of the ratios $c_{h1}^{(1)}/c_{h0}^{(1)}$ and $\bar{u}_{sl}^{(1)}/\bar{u}_{top}^{(1)}$. Thus, these ratios may be used to develop design charts.

Author Contributions Amitava Chakraborti and Dipanjan Basu contributed to the conceptualization and analysis of the research study. All authors contributed to writing and editing of the manuscript. All authors read and approved the final manuscript.

Data Availability Statement Data from numerical simulations will be made available upon reasonable request.

References

- Johnson SJ (1970) Foundation precompressions with vertical sand drains. *Proc Am Soc Civil Eng Conf Place Improv Soil Support Struct* 96:9–42
- Holtz RD (1987) Preloading with prefabricated vertical strip drains. *Geotext Geomembr* 6:109–131
- Bergado DT, Alfaro MC, Balasubramaniam AS (1993) Improvement of soft Bangkok clay using vertical drains. *Geotext Geomembr* 12:567–586
- Bo MW, Chu J, Low BK, Choa V (2003) Soil improvement: prefabricated vertical drain technique. Thomson Learning, Singapore
- Qi C, Li R, Gan F, Zhang W, Han H (2020) Measurement and simulation on consolidation behaviour of soft foundation improved with prefabricated vertical drains. *Int J Geosynth Gr Eng* 6:23
- Badarinath R, El Naggari H (2021) Improving the stability of high embankments founded on soft marine clay by utilizing prefabricated vertical drains and controlling the pace of construction. *Int J Geosynth Gr Eng* 7:68
- Barron RA (1948) Consolidation of fine grained soils by drain wells. *Trans Am Soc Civil Eng* 113(2346):718–754
- Kjellman W (1948) Accelerating consolidation of fine grained soils by means of cardboard wicks. In: *Proceedings of Second International Conference on Soil Mechanics and Foundation Engineering, II, Rotterdam*, pp 302–305
- Basu D, Madhav MR (2000) Effect of prefabricated vertical drain clogging on the rate of consolidation: a numerical study. *Geosynth Int* 7(3):189–215
- Casagrande L, Poulos S (1969) On the effectiveness of sand drains. *Can Geotech J* 6(3):287–326
- Hansbo S (1981) Consolidation of fine grained soil by prefabricated drains. *Proc Int Conf Soil Mech Found Eng* 3:677–682
- Hansbo S (1986) Preconsolidations of soft compressible sub soil by the use of prefabricated vertical drains. *Ann des Trav Publics de Belgique* 6:553–563
- Hansbo S (1987) Design aspects of vertical drains and lime column installations. In: *Proceedings of 9th Southeast Asian geotechnical conference, Bangkok*, pp 1–12
- Bergado DT, Asakami H, Alfaro MC, Balasubramaniam AS (1991) Smear effects of vertical drains on soft Bangkok clay. *J Geotech Eng ASCE* 117(10):1509–1530
- Indraratna B, Redana IW (1997) Plain strain modelling of smear effects associated with vertical drains. *J Geotech Geoenviron Eng ASCE* 123(5):474–478
- Chai JC, Miura N (1999) Investigation of factors affecting vertical drain behavior. *J Geotech Geoenviron Eng* 125(3):216–226
- Chu H, Yan S, Indraratna B, Rujikiatkamjorn C (2014) Overview of preloading methods for soil improvement. *Proc Instit Civil Eng Gr Improv* 167(G13):173–185
- Welker AL, Gilbert RB, Bowders JJ (2000) Using a reduced equivalent diameter for a prefabricated vertical drain to account for smear. *Geosynth Int* 7(1):47–57
- Prabavathy S, Rajagopal K, Pitchumani NK (2021) Investigation of smear zone around PVD mandrel using image-based analysis. *Int J Geosynth Gr Eng* 7:94
- Madhav MR, Park Y-M, Miura N (1993) Modelling and study of smear zones around band shaped drains. *Soils Found* 33(4):135–147
- Indraratna B, Redana IW (2000) Numerical modelling of vertical drains with smear and well resistance installed in soft clay. *Can Geotech J* 37:133–145
- Sharma JS, Xiao D (2000) Characterization of a smear zone around vertical drain by large scale Laboratory test. *Can Geotech J* 37(6):1265–1271
- Basu D, Prezzi M (2009) Design of prefabricated vertical drains considering soil disturbance. *Geosynth Int* 16(3):147–157
- Basu D, Prezzi M (2007) Effect of smear and transition zones around prefabricated vertical drains installed in a triangular pattern on the rate of consolidation. *Int J Geomech ASCE* 7(1):34–43
- Holtz RD, Jamiolkowski MB, Lancellotta R, Pedroni R (1991) Prefabricated vertical drains: design and performance. Butterworth-Heinemann, Oxford
- Basu D, Basu P, Prezzi M (2006) Analytical solutions for consolidation aided by the vertical drains. *Geomech Geoeng* 1(1):63–71
- Walker R, Indraratna B (2007) Vertical drain consolidation with overlapping smear zones. *Geotechnique* 57(5):463–467
- Rujikiatkamjorn C, Indraratna B (2009) Design procedure for vertical drains considering a linear variation of permeability within the smear zone. *Can Geotech J* 46:270–280
- Nghia NT, Lam LG, Shukla SK (2018) A new approach to solution for partially penetrated prefabricated vertical drains. *Int J Geosynth Gr Eng* 4:11
- Barron RA (1944) The influence of drain wells on the consolidation of fine-grained soils. *Diss. Providence US Engineering Office*.
- Yoshikuni H, Nakanodo H (1974) Consolidation of soils by vertical drain wells with finite permeability. *Soil Found* 14(2):34–45
- Tanaka Y (1998) Vertical drains for layered clay strata. In: *Proceedings of International Offshore Polar Engineering Conference*, pp 478–483
- Tang XW, Onitsuka K (2001) Consolidation of double-layered ground with vertical drains. *Int J Numer Anal Meth Geomech* 25:1449–1465
- Tang X, Niu B, Cheng G, Shen H (2013) Closed-form solution for consolidation of three-layer soil with a vertical drain system. *Geotext Geomembr* 36:81–91
- Liu J-C, Lei G-H, Zheng M-X (2014) General solutions for consolidation of multilayered soil with a vertical drain system. *Geotext Geomembr* 42:267–276
- Indraratna B, Geng XY, Rujikiatkamjorn C (2012) Consolidation of ground with prefabricated vertical drains combined with time-dependent surcharge loading in membrane system. In: *Proceedings GeoCongress 2012, ASCE*, pp 60–69
- Deng YB, Liu GB, Indraratna B, Rujikiatkamjorn C, Xie K-H (2017) Model test and theoretical analysis for soil foundation improved by prefabricated vertical drains. *Int J Geomech ASCE* 17(1):1–12
- Long R (1990) Techniques of back figuring consolidation parameters from field data. *Transp Res Rec* 1277:71–79
- Das BM (2014) *Advanced soil mechanics*, 4th edn. CRC Press, London
- Welker AL, Herdin KM (2003) Evaluation of four equivalent diameter formulations for prefabricated vertical drains using flow rates. *Geosynth Int* 10(3):103–109
- Leo CJ (2004) Equal strain consolidation by vertical drains. *J Geotech Geoenviron Eng ASCE* 130(3):316–327
- Seah TH, Tangthansup B, Wongsatian P (2004) Horizontal coefficient of consolidation of soft Bangkok clay. *Geotech Test J* 27(5):430–440
- Lim GT, Pineda JA, Boukpeti N, Cararo JAH (2018) Predicted and measured behaviour of an embankment on PVD-improved Ballina clay. *Comput Geotech* 93:204–221

Publisher's Note Springer Nature remains neutral with regard to jurisdictional claims in published maps and institutional affiliations.